DMD Fast Forward. Published on April 25, 2018 as DOI: 10.1124/dmd.118.080457
This article has not been copyedited and formatted. The final version may differ from this version.

Metabolism of a $5HT_6$ antagonist, 2-methyl-1-(phenylsulfonyl)-4-(piperazin-1-yl)-1H-benzo[d]imidazole (SAM-760): impact of sulfonamide metabolism on diminution of a ketoconazole mediated clinical drug-drug interaction

Aarti Sawant-Basak*, R. Scott Obach, Angela Doran, Peter Lockwood, Klaas Schildknegt, Hongying Gao, Jessica Mancuso, Susanna Tse, and Thomas A. Comery.

Pfizer Worldwide Research & Development, Pharmacokinetics, Dynamics & Metabolism (PDM), 1 Portland Street, Cambridge MA 02139 (A.S-B); Pfizer Worldwide Research & Development, Pharmacokinetics, Dynamics & Metabolism (PDM), Groton, CT 06340 (R.S.O., A.D., H.G., S.T.); Pfizer Global Product Development, Groton, CT 06340 (P.L.); Pfizer Worldwide Research & Development Pharmaceutical Sciences Chemical Research and development, Groton CT 06340 (K.S.); Pfizer Worldwide Research and Development, Research Statistics, 1 Portland Street, Cambridge MA 02139 (J.M.); Pfizer Neuroscience and Pain Research Unit, Worldwide Research and Development, 610 Main Street, Cambridge, MA 02139 (T.C.).

Running Title: Novel sulfonamide metabolite explains ketoconazole DDI

Address correspondence to:

Aarti Sawant-Basak, Ph.D.

Pharmacokinetics, Dynamics, and Metabolism

Worldwide Research and Development

Pfizer Inc.

1 Portland Street, Kendall Square,

Cambridge, MA 02139

Tel. 617.395.0758

Email: aarti.sawant@pfizer.com

Text pages: 26

Tables: 3

Figures: 6

References: 18

Words in Abstract: 249

Words in Introduction: 461

Words in Discussion: 1,333

DMD Fast Forward. Published on April 25, 2018 as DOI: 10.1124/dmd.118.080457
This article has not been copyedited and formatted. The final version may differ from this version.

Abbreviations: SAM-760, (2-methyl-1-(phenylsulfonyl)-4-(piperazin-1-yl)-1H-benzo[d]imidazole); $5HT_6$: serotonin receptor subtype 6; [^{14}C] SAM-760, radioactive carbon isotope labeled SAM-760; non-CYP, non-cytochrome P450; AD, Alzheimer's disease; C_{max}, maximal plasma concentration achieved; $AUC_{0\text{-}inf}$, area under the plasma concentration-time curve from time zero extrapolated to infinite time; DDI, drug-drug interaction; 1-ABT, 1-Aminobenzotriazole; HCOOH, formic acid; CH_3CN, acetonitrile; ESI, electrospray ionization; MIM-EPI, multiple ion monitoring enhanced product scan; MRM-EPI, multiple reaction monitoring enhanced product scan; f_mCYP is the fraction of metabolism catalyzed by specific CYP; $f_{CL,}$ fraction of total clearance; IS internal standard; MeOH, methanol; LLOQ, lower limit of quantitation; BLQ, below the limit of quantitation; $F_{g,}$ fraction escaping the gut; $F'_{g,}$ fraction escaping the gut in presence of the inhibitor; HLMs, human liver microsomes; CL/F, total oral clearance; GSH, glutathione; GST, glutathione transferase; NAT, N-acetyl transferase; cps, counts per second; SEM, standard error of the mean; WEM, William's E Media

Abstract. SAM-760, (2-methyl-1-(phenylsulfonyl)-4-(piperazin-1-yl)-1H-benzo[d]imidazole), a $5HT_6$ antagonist, was investigated in humans for the treatment of Alzheimer's dementia. In liver microsomes and recombinant CYP450 isozymes, SAM-760 was predominantly metabolized by CYP3A (~85%). Based on these observations and an expectation of 5-fold magnitude of interaction with moderate to strong CYP3A inhibitors, a clinical DDI study was performed. In presence of ketoconazole, mean C_{max} and $AUC_{0–inf}$ of SAM-760 showed only a modest increase by 30% and 38%, respectively. In vitro investigation of this unexpectedly low interaction was undertaken using [^{14}C]SAM-760. Radiometric profiling in human hepatocytes, confirmed all oxidative metabolites previously observed with unlabeled SAM-760; however the predominant radiometric peak was an unexpected polar metabolite which was insensitive to pan-CYP inhibitor, 1-aminobenzotriazole. In human hepatocytes, radiometric integration attributed 43% of total metabolism of SAM-760 to this non-CYP pathway. Using an authentic standard, this predominant metabolite was confirmed as benzenesulfinic acid. Additional investigation revealed that the benzenesulfinic acid metabolite may be a novel, non-enzymatic, thiol mediated reductive cleavage of aryl sulfonamide group of SAM-760. We also determined the relative contribution of P450 to metabolism of SAM-760 in human hepatocytes, by following the rate of formation of oxidative metabolites in presence and absence of P450 isoform specific inhibitors. P450 mediated oxidative metabolism of SAM-760 was still primarily attributed to CYP3A (33%), with minor contributions from CYP isoforms 2C19 and 2D6. Thus, disposition of [^{14}C]SAM-760 in human hepatocytes via novel sulfonamide metabolism and CYP3A

verified the lower than expected clinical DDI when SAM-760 was co-administered with ketoconazole.

DMD Fast Forward. Published on April 25, 2018 as DOI: 10.1124/dmd.118.080457
This article has not been copyedited and formatted. The final version may differ from this version.

Introduction

Alzheimers' Disease is a progressive neuro-degenerative disorder characterized by a decline in cognitive and functional abilities. It is the most common cause of dementia, with limited standards of care. The current pharmacotherapy for AD involves acetylcholinesterase inhibitors (e.g., donepezil and rivastigmine), which increase cholinergic tone throughout the brain by inhibiting the catabolism of acetylcholine via inhibition of esterase activity. While not disease modifying, these cause symptomatic relief and improvement of cognition over the shorter term treatment. Therefore adjunct therapies targeting receptors of complimentary mechanisms regulating the release of additional neurotransmitters like glutamate and serotonin may provide a new mechanism to increase the therapeutic potential of donepezil. One of these targets gaining recent attention was the $5HT_6$ receptor which is a G-protein-coupled receptor (GPCR) expressed in brain regions critical for cognitive functioning and is positively coupled to adenylate cyclase. Micro-dialysis in rat cortex and hippocampus has shown that 5-HT_6 receptor antagonism stimulates extracellular acetylcholine and glutamate release as well as enhances cognition and improves memory deficits in rodent models (Hirst et al., 2006; Foley et al., 2008). Early stage clinical trials had illustrated the potential application of 5-HT_6 antagonists as an adjunct to donepezil in symptomatic treatment of AD (Maher-Edwards et al., 2011). Consistent with this rationale, drug design efforts led to identification of SAM-760 (Haydar, 2009; Liu et al., 2011) **(Figure 1)**, as a potential clinical 5-HT_6 antagonist, with projected efficacy at 50 mg/day. Prior to administration of SAM-760 in humans, preliminary investigation of its major clearance mechanisms suggested that the main route of clearance was via oxidative metabolism

of the piperazine core, including N-dealkylation. Substrate depletion kinetics of SAM-760 using human liver microsomes and recombinant P450 isozymes showed that metabolic clearance was predominantly (~85%) via CYP3A. Therefore, during phase 1 clinical development, the effects of ketoconazole, a strong CYP3A inhibitor, were studied on the pharmacokinetics of SAM-760. This clinical drug-drug interaction (DDI) study showed a 1.38 fold increase in plasma AUC_{0-inf} of SAM-760, in presence of ketoconazole. This low magnitude of pharmacokinetic interaction was unexpected based on the f_m value of ~0.85. As a result, deeper investigation of clearance mechanisms of SAM-760 was conducted using radiolabeled material in a comprehensive metabolic system (i.e. human hepatocytes). This paper describes the results of this investigation of [^{14}C]SAM-760. We report a previously unreported aryl sulfonamide cleavage pathway of SAM-760 which was subject to further mechanistic investigation. In addition, we also determined the exact contribution of CYP3A via metabolite formation kinetics in human hepatocytes using P450 isozyme specific inhibitors to verify CYP3A victim drug-drug interaction. This research exemplifies the importance of using radiolabeling compounds for deeper investigational studies of low turnover compounds and the use of complete in vitro systems towards accurate prediction of disposition and victim based DDI of new clinical candidates.

Materials and Methods

[^{14}C]SAM-760 was synthesized as described below. SAM-760 was synthesized at Pfizer research laboratories (Haydar, 2009). WYE-103760 D_8 was obtained from Wyeth Research Laboratories, Pearl River, NY. Cryopreserved human hepatocytes (lot RTH) prepared as a mixture of 10 donor livers (7 females and 3 males) were purchased from Celsis InVitro Technologies (Baltimore, MD). All solvents and buffers were of HPLC grade and procured from J.T. Baker (Pittsburgh, PA). Furafylline, 1-aminobenzotriazole, ticlopidine, and mibefradil were purchased from Sigma-Aldrich Co (St. Louis, MO, USA). Paroxetine was obtained from Sequoia Research Products (Pangborne, United Kingdom) and tienilic acid from Xenotech (Kansas City, KS). All other reagents were the highest grade commercially available. All clinical studies were conducted in compliance with the ethical principles originating in or derived from the Declaration of Helsinki and in compliance with all International Conference on Harmonization Good Clinical Practice Guidelines and the International Ethical Guidelines for Biomedical Research Involving Human Subjects (Council for International Organizations of Medical Sciences 2002). All local regulatory requirements were followed, in the interest of greater protection to the safety of study participants.

Synthesis of [^{14}C]SAM-760:

Preparation of [^{14}C]*t*-butyl 4-(2-methyl-1-(phenylsulfonyl)-1H-benzo[*d*]imidazol-4-yl)piperazine-1-carboxylate (2).

A solution of **1** (593 mg, 1.87 mmol) and Hunig's base (0.39 mL, 2.25 mmol) in 4 mL of isopropyl acetate was treated with a solution of [^{14}C]benzenesulfonyl chloride (150 mCi, 80 mCi/mmol, 1.87 mmol) in 2 mL of isopropyl acetate. The reaction was heated at 65

°C for 2 hours and then cooled to room temperature and partitioned between 5 mL of water and 5 mL of isopropyl acetate. The organic layer was washed with 5 mL of water and concentrated to afford an oil. The oil was diluted with 3 mL of isopropyl acetate and 6 mL of heptane and seeded at room temperature with non-labeled **2**. The resulting suspension was cooled to 0 °C and filtered, rinsing with heptane. The collected product was air-dried to give **2** (564 mg, 1.23 mmol, 66% yield) as a white solid.

Preparation of [^{14}C]SAM-760.

A suspension of **2** (564 mg, 1.23 mmol) in 3 mL of toluene was cooled to 0 °C and treated with trifluoroacetic acid (0.95 mL, 12.3 mmol). The resulting biphasic mixture was stirred at room temperature for 2.5 hours. A mixture of concentrated ammonium hydroxide (1.7 mL, 12.3 mmol) in 10 mL of isopropyl acetate was added and the reaction was stirred for an additional 2 hours. The resulting biphasic mixture was treated with 5 mL of 5% aq K_2CO_3 and the layers were separated. The organic layer was washed with 5 mL of 5% aq K_2CO_3 followed by 2 x 10 mL of water. The organic layer was concentrated to afford an oil and this was diluted with 2 mL of isopropyl acetate and 3.5 mL of heptane. The resulting suspension was cooled to 0°C and filtered, rinsing with heptane. The collected product was air-dried to give **[^{14}C]SAM-760** (324 mg, 0.90 mmol, 73% yield) as a white solid A summary of radiolabeled synthesis is depicted in **Scheme 1**.

Incubation of [^{14}C]SAM-760 in human hepatocytes for metabolite identification in presence and absence of 1-ABT. Hepatocytes were thawed as per supplier's protocol. Thawed hepatocytes were suspended in WEM medium, and cells were counted for

viability, using the trypan blue exclusion method. After meeting an internal acceptance criteria of >85% viability of the total number of cells, the hepatocyte suspension were diluted in WEM to achieve the desirable cell concentration (i.e. 0.75 million cells/mL). A mixture of radiolabeled ([^{14}C] SAM-760, 6.7 mCi/mmol) and unlabeled SAM-760 (10 μM) was incubated with cryopreserved human hepatocytes diluted to 0.75 million cells/mL in WEM at 37^{o}C under an atmosphere of O_2/CO_2 (95/5) and in a final incubation volume of 1.5 mL. Samples were shaken on a rotating platform at 200 rpm, in an incubator. CYP450 metabolism was quantitatively assessed by conducting incubations of SAM-760 in cryo-preserved hepatocytes in presence or absence of the pan-CYP inhibitor, 1-ABT. Experiments containing 1-ABT were conducted by a 30-minute pre-incubation of cryopreserved hepatocytes with 1-ABT prior to addition of 10 μM SAM-760). Incubations were terminated by addition of 50 μL of 0.1% HCOOH after 0 and 4 hr. The mixtures were centrifuged and supernatants were analyzed, using HPLC followed by radiometry and mass spectrometry (see below). Incubations were performed in triplicates.

HPLC-MS and Radiometric analysis of [^{14}C] SAM-760. Terminated incubation mixtures were injected (0.1 mL) onto a Varian Polaris C_{18} column (4.5 x 250 mm; 5 μm) in a mobile phase consisting of 0.1% HCOOH in CH_3CN (10%) at a flow rate of 0.8 mL/min. This composition was maintained for 5 min followed by a linear gradient to 50% CH_3CN at 50 min, a 10 min wash at 95% CH_3CN, and a 10 min re-equilibration time, at initial conditions. The effluent was split between a fraction collector and a Thermo Finnigan LTQ ion trap mass spectrometer, (split ratio was ~1:15). The MS was operated in the positive ion mode, with tuning parameters and potentials optimized to

maximize the signal for the protonated molecular ion of SAM-760. Fractions were collected every 20 sec into 96-well Scintiplates (Perkin–Elmer, Waltham, MA) and subjected to vacuum centrifugation to remove the solvent. The dried plates were counted in a MicroBeta scintillation counter, (3 min counting time). The radio-chromatograms from individual incubations were averaged; % of each of the metabolites was calculated by manual integration of the averaged radiometric peaks of individual metabolite and normalized to total radioactivity in the incubations.

Inhibition of SAM-760 metabolism in human hepatocytes using P450 isozyme specific inhibitors. In a preliminary experiment, it was shown that the metabolite profile at substrate concentrations of 1 and 10 µM was the same and that there was approximately 10-fold greater abundance of all metabolites of SAM-760 at 10 µM vs 1 µM. Therefore all subsequent experiments were carried out at a substrate concentration of 10 µM. Thus, SAM-760 (10 µM) was incubated with cryopreserved human hepatocytes (0.75 million cells/mL) in the presence or absence of CYP selective inhibitors. The incubations (N=3) were conducted in 24-well cell culture plates at 37^{o} C in a CO_2 incubator under an atmosphere of O_2/CO_2 (95/5). Human hepatocytes were pre-incubated for 30 minutes with CYP selective time-dependent inactivators of CYP1A2 (1 µM furafylline), CYP2C9 (10 µM tienilic acid), CYP2C19 (30 µM ticolpidine), CYP2D6 (2 µM paroxetine), and CYP3A4/5 (10 µM mibefradil) prior to the addition of SAM-760. The reactions were terminated after one hour of incubation by transferring aliquots to a clean 96-well plate and centrifuging for 3 min at 50 g. The resulting

supernatants were transferred to a clean 96-well plate containing internal standard (250 ng/mL metoprolol and terfenadine) and were stored at -80°C prior to analysis.

Semi-quantitative analysis of metabolites in chemical inhibition samples, using HPLC-MS/MS.

Liquid chromatography separation was performed on a Kinetex C-18 (2.1 x 50 mm 107 µm) coupled to a Waters Acquity UPLC. The mobile phase B was acetonitrile and the aqueous mobile A phase was prepared with Formic Acid acid at 0.1 % concentration. The flow rate for all experiments was 0.5 mL/min. The sample was injected using a linear gradient of 2% B (0.1% formic acid/acetonitrile) by Aquity autosampler (Waters, MA, USA) with a 5.0µL injection volume for total of 3 minute run time. Chemical inhibition samples were injected (5.0 µL) onto a Phenomenex Kinetex C_{18} column (2.1 x 50-mm, 1.7-µm) in an initial mobile phase composition of 98% of 0.1% HCOOH in water (A), and 2% of 0.1% HCOOH in acetonitrile (B) at a flow rate of 0.5 mL/min for 0.5 min. This was followed by consecutive linear gradients of 1.5 min to 60% B and then 18 sec to 90% B where it was held for 12 sec. An 18 sec linear gradient returned the column to the initial composition where the column was re-equilibrated for 12 sec. Mass spectrometric semi-quantitative experiments were performed on an AB Sciex API5500 QTRAP mass spectrometer in the positive electrospray ionization (ESI) mode. Semi-quantitative methods, for quantitating CYP450-sensitive metabolites in chemical inhibition studies, were developed by injecting samples generated from a pilot study where unlabeled SAM-760 was incubated with hepatocytes. The metabolites generated in this pilot experiment were determined using multiple ion monitoring-enhanced product ion scans (MIM-EPI) scans to qualitatively confirm the identity and establish the

retention time of the metabolites relative to those observed in the biotransformation studies with radiolabeled material. Product ions were generated for the most intense parent ion with a response greater than 5000-cps after dynamic background subtraction. A semi-quantitative MRM-EPI method was then created for sample analysis by linking the parent ion with the most intense product ion. MRM responses greater than 5000-cps after dynamic background subtraction triggered EPI scans to qualitatively confirm the identification of the metabolite and MRM metabolite/internal standard peak area ratios were used to determine the percent inhibition. Triggered EPI scans were collected at collision energies of 50, 40, and 30-eV with a scan rate of 20,000-Da/s. The MRM transitions and retention times of the analytes are listed in **Table 2**. The following mass-independent, mass-spectrometer parameters were applied to detect SAM-760 and the test compounds: collision energy 35-eV for MRM transitions, de-clustering potential 50-V, temperature 450^{o} C, IS voltage 4500-V, dwell time 2.0-ms, and collision gas set at medium. Analyst version 1.5.1 (AB Sciex) was utilized to control the LC-MS/MS system, collect data and perform data reduction. Since the measured metabolites would be in a linear dynamic range, this semi-quantitative method was considered to be adequate for measuring metabolites from the chemical inhibition study.

Data Analysis.

In order to estimate the overall contribution of individual CYP enzymes to the overall metabolism of SAM-760, a 3-step process was conducted. First, the fraction of overall metabolism of [^{14}C]SAM-760 to each individual metabolites was calculated from the radio-chromatogram data as follows:

Equation 1:

$$\frac{\text{radioactivity in metabolite X peak}}{\text{total radioactivity in chromatogram}} = f_{CL(\text{metabolite X})}$$

Next, the LC-MS-MS MS peak area ratios of each of the metabolites in chemical incubations (of unlabeled SAM-760 in human hepatocytes with and without specific P450 inhibitors) were determined. The fraction of control for a metabolite X using an inhibitor of "CYP #1" was calculated by:

Equation 2:

$$\frac{\text{peak area of metabolite X in presence of inhibitor}}{\text{peak area of metabolite X in no inhibitor control}} = f_{control(\text{metabolite X, CYP\#1})}$$

Then, the contribution of CYP#1 to the total metabolism of SAM-760 was calculated by summing the metabolic contributions of all metabolites generated by CYP#1 as follows:

Equation 3:

$$f_{CL,SAM\text{-}760(CYP\#1)} = f_{CL(\text{metabolite X})} \bullet f_{control(\text{metabolite X, CYP\#1})} + f_{CL(\text{metabolite Y})} \bullet f_{control(\text{metabolite Y, CYP\#1})} + \cdots\cdots$$

Thus the fractions of SAM-760 metabolized by specific CYP isoforms (f_m) were determined by integrating results from chemical inhibition studies into the HPLC-radio-chromatographic measurements. The fraction of clearance determined was converted to % contribution of individual CYPs.

Incubation of SAM-760 with thiols. SAM-760 (200 µM) was incubated with GSH (5 mM), N-acetylcysteine (5 mM), β-mercaptoethanol (100 mM), or no thiol (control) in 1 mL of 100 mM potassium phosphate at pH 7.5 at 37^{o}C. These reaction mixtures were directly injected (0.02 mL) onto a Waters HSS T3 UHPLC column (2.1 x 100 mm; 1.7 µ) equilibrated in 10 mM aqueous ammonium acetate at a flow rate of 0.4 mL/min. This mobile phase condition was held for 0.5 min followed by a linear increase to 80%

DMD Fast Forward. Published on April 25, 2018 as DOI: 10.1124/dmd.118.080457
This article has not been copyedited and formatted. The final version may differ from this version.

acetonitrile at 5 min, held for 1 min, and re-equilibrated to initial conditions for 1 min. The effluent was introduced into a Thermo Orbitrap Elite high resolution mass spectrometer operated in the negative ion full MS1 scan mode. Source temperatures and potentials were adjusted to optimize the signal for benzenesulfinic acid, which eluted at 2.7 min.

Human plasma pharmacokinetics of oral SAM-760 administered with or without ketoconazole. On day 1, Period 1 comprising of (N=12) healthy, young, male subjects received a single 5 mg dose of SAM-760 after an overnight fast of at least 10 hours. In Period 2, from Day -2 to Day 12 (a total of 14 days), each subject received a daily dose of ketoconazole 400 mg QD (2 x 200-mg tablets). In Period 2, Day 12, a single 5 mg dose of SAM-760 was co-administered (with ketoconazole) after an overnight fast of at least 10 hours. Blood samples (5 mL) were obtained -1, 0.5, 1, 1.5, 2, 3, 4, 6, 8, 10, 12, 16, 24, 36, 48, 72, and 96 hours after SAM-760 administration and centrifuged. EDTA plasma was harvested by centrifugation (3000 g for 10 min) of whole blood at 4 ºC. Samples were stored at -20 ºC until further processing or analysis.

Quantification of SAM-760 in human plasma. A validated LC-MS/MS method quantitated SAM-760 in human EDTA plasma. The method utilized an automated solid phase extraction procedure prior to LC-MS/MS analysis. A stable isotope-labeled version of SAM-760, WYE-103760 D_8 **(Figure 1)**, was used as the internal standard (IS). Linearity of SAM-760 in human plasma was observed over the concentration range of 0.250 to 500 ng/mL, using a plasma sample volume of 0.100 mL. Reconstituted extracts of EDTA plasma were analyzed by LC-MS/MS. A 5.0 min gradient was used to achieve separation using Applied Biosystems API 4000 system using a binary pump to

deliver mobile phase. Extracts were injected (10 µL) onto an Echelon C_{18} column (30 mmx2.1 mm, 4 µM), equilibriated in MeOH/ACN/H_2O/0.1%formic acid (10/10/80) at a flow rate of 0.4 mL/min for 0.5 min, followed by a change in gradient from 0.5 to 1.6 min to MeOH/ACN/H_2O/formic acid (40/50/10/0.1 v/v). The gradient was held from 1.6 min to 3.8 min and then equilibrated to starting conditions from 3.8 to 5 min. SAM-760 and internal standard (IS) were detected in positive ion electrospray using multiple-reaction monitoring mass transitions for SAM-760 (*m/z* 357.16→216.15) and IS (*m/z* 365.12→224.10). The dynamic range of the assay was from 0.05 to 1000 ng/mL. Peak-area integrations were performed using MDS Sciex/Applied Biosystems Analyst software (version 1.4.2 or successor system).

Pharmacokinetic calculations. Pharmacokinetic parameters of SAM-760 were derived from plasma concentration-versus-time profile. Plasma PK parameters of SAM-760 (C_{max} and AUC_{0-inf}) were calculated using version 2.2.2. eNCA which is a proprietary global repository for pharmacokinetic (PK) concentration and NCA parameter data as well as the global system for generating non compartmental analyses. Samples below the LLOQ (0.25 ng/mL) were set to 0 ng/mL for data analysis.

Results

Metabolism of [^{14}C]SAM-760 in cryopreserved human hepatocytes. [^{14}C]SAM-760 (labeled on the aryl ring system, **Figure 1**) was incubated in human hepatocytes for t=0 (control) and t=4h. The incubation mixtures were assessed using HPLC followed by radiometric assessment as well as mass spectrometry and are depicted in **Figure 2** as blue (control) and red (t=4h) traces. The green trace in **Figure 2** represents [^{14}C]SAM-

760 (10 µM) incubated with human hepatocytes and 1 mM 1-ABT. SAM-760 showed a slow rate of metabolism in human hepatocytes over 4h of incubation as observed from the radio-chromatogram (red trace) where the largest radioactive peak belonged to the parent compound (R_t ~35 min). The peaks eluting at R_t ~ 14 and ~26 min (designated with "i" in **Figure 2**) represent radiochemical impurities and were not included in data analysis. Metabolite peaks observed in this radiometric HPLC analysis have been designated as peaks 1 to 15 and their proposed structures are shown in **Figure 3** and described below; wherever possible metabolites were confirmed by co-elution with authentic standards which were biosynthesized (methods not shown), or commercially purchased.

Several drug metabolism reactions contributed to the fifteen metabolite peaks observed from incubation of [^{14}C] SAM-760 in human hepatocytes. Peaks arose via hydroxylation, N-oxidation, piperazine oxidation, N-sulfation, and reductive sulfonamide cleavage **(Figure 3)**. Peak 1 which was broad and polar, (eluted earlier than the parent, on the C_{18} column; R_t ~ 15 min), was the most abundant metabolite peak, and was of significant interest as it represented the predominant metabolic pathway of SAM-760 in human hepatocytes. In positive ion electrospray it corresponded to *m/z* 143 and fragmented to predominant daughter ions of *m/z* 125 and *m/z* 79, corresponding to a loss of water molecule and 64 amu, respectively. While the peak of *m/z* 125 did not reveal significant information, the loss of 64 amu from *m/z* 143 was suggestive of a loss of $–SO_2$ from the molecule; the resulting stable daughter ion of *m/z* 79 corresponded to a benzylium species further suggesting that *m/z* 143 could be benzene sulfinic acid arising from the aryl sulfonamide moiety of SAM-760. Based on mass of *m/z* 143 and

DMD Fast Forward. Published on April 25, 2018 as DOI: 10.1124/dmd.118.080457
This article has not been copyedited and formatted. The final version may differ from this version.

co-elution of Peak 1 with an authentic standard, it was confirmed to be benzenesulfinic acid **(Figure 4).** Peaks 2 and 4 were present at 6.3 and 1.9% of metabolism, respectively but were not identified, as no mass spectral data were observed for either of them.

Almost all of the remaining peaks arose via oxidation reactions including hydroxylation on the benzimidazole ring (peaks 5 and 6), N-hydroxylation of the 2^o piperazine nitrogen (peak 9), and oxidative ring-opening reactions of the piperazine (peaks 7, 11, 14, and 15). Peak 3 was identified as the glucuronidated conjugate of peak 5/6 and Peak 13 was proposed to be an N-acetyl conjugate of the piperazine ring oxidation product. Peak 12 was identified as the sulfamic acid conjugate of the 2^o piperazine nitrogen. In conclusions, SAM-760 metabolized to several primary and secondary metabolites when incubated in human hepatocytes; predominant pathway of metabolism was identified as cleavage of the imidazole sulfonamide, to form benzenesulfinic acid.

Contribution of P450 and non-P450 mediated metabolism of ^{14}C SAM-760 in human hepatocytes. Formation of benzenesulfinic acid and its contribution to total metabolic clearance was determined by incubation of [^{14}C]SAM-760 in presence (green trace) and absence of 1 mM 1-ABT (red trace). Formation of peak 1 was not sensitive to presence of 1 mM 1-ABT demonstrating that this was a non-P450 mediated clearance mechanism. The contribution of each metabolic pathway (% of metabolism) to the overall clearance of SAM-760 was determined by dividing the radiometric response of an individual metabolite by the sum of all drug-related radiometric metabolite peaks identified in the study. Benzenesulfinic acid metabolite was calculated to be 43% of total

metabolism further confirming that it was indeed the major biotransformation route of clearance of SAM-760. After quantitating the sulfinic acid metabolite, all other metabolites represented between 1 and 12 were calculated as % of total metabolism. Amongst the remaining routes of clearance, the piperazine sulfamic acid metabolite was attributed to be 4.5% of total metabolic clearance, suggesting that remaining ~40-45% of metabolic clearance could be P450 mediated **(Table 1)**.

P450 reaction phenotyping in human hepatocytes using P450 specific inhibitors. As determined above, P450 mediated metabolism contributed to ~40-45 % of total metabolic clearance **(Table 1)**. The contribution of CYP3A towards total P450 mediated metabolism of SAM-760, was determined by incubation of SAM-760 in human hepatocytes in presence or absence of P450 selective inhibitors. To determine the CYP contribution to each specific metabolic pathway of SAM-760 in human hepatocytes, the relative change in metabolite formation in the presence or absence of CYP selective inhibitor was calculated using **Equations 1-3**. Incubation of SAM-760 in human hepatocytes in presence or absence of P450 selective inhibitors ticlopidine, paroxetine, and mibefradil indicated that CYPC19, CYP2D6, and CYP3A4/5 contributed to P450 mediated metabolism of SAM-760. There were no inhibitory effects on formation of any of the metabolites by furafylline (CYP1A2 inactivator) or tienilic acid (CYP2C9 inhibitor). Inhibition by mibefradil was observed on peaks 3, 8, 9, 13, 14, and 15. In addition to mibefradil, peaks 6, 7, 10 and 11 were also inhibited by ticlopidine; peak 5 was inhibited by paroxetine. Results are summarized in **Table 2**. In human hepatocytes, the oxidative metabolism of SAM-760 was predominantly attributed to CYP3A (33%), with minor contributions by CYP2C19 (6.3%) and CYP2D6 (0.47%). P450 mediated metabolism

accounted for up to 39.8% of the total clearance pathways of SAM-760, with CYP3A playing a major role in oxidative metabolism.

Incubation of SAM-760 with thiol reagents. 200 µM SAM-760 was incubated in buffer (pH 7.5) with GSH (5 mM), N-acetylcysteine (5 mM), β-mercaptoethanol (100 mM), or no thiol (control). Incubations were injected onto LC-MS/MS under negative ion electrospray ionization. The presence of benzene sulfinic acid in incubations containing a thiol but not in the control was observed (**Figure 5**). This suggested that the observation of benzene sulfinic acid in hepatocyte incubation of SAM-760 likely arises by chemical reduction of aryl sulfonamide bond of SAM-760 by glutathione or other thiols present in the incubations.

Pharmacokinetics of SAM-760 in healthy volunteers in presence and absence of ketoconazole. Healthy, male volunteers were administered a single oral dose of SAM-760 (5 mg) alone or with ketoconazole (400 mg). Mean exposures of SAM-760 following a single 5 mg oral dose (C_{max} 3.43 ng/mL and $AUC_{0–inf}$ 154.5 ng*h/mL) increased (C_{max} 4.47 ng/mL and $AUC_{0–inf}$ 213.7 ng*h/mL), when it was co-administered with ketoconazole **(Table 3 and Figure 6)**. Thus, in the presence of ketoconazole, mean plasma C_{max} and $AUC_{0\text{-}inf}$ of a single oral dose of 5 mg dose of SAM-760 increased by 30% and 38%, respectively.

DMD Fast Forward. Published on April 25, 2018 as DOI: 10.1124/dmd.118.080457
This article has not been copyedited and formatted. The final version may differ from this version.

Discussion

Prior to administration of a new drug candidate to humans, drug-drug interactions (inhibition of clearance pathways of a compound resulting in increased exposure) could be predicted with reasonable confidence by integrating in vitro clearance estimations and fraction metabolized, or less frequently, in vivo animal studies (Kotegawa et al., 2002; Vuppugalla et al., 2012). If there is high confidence that all human clearance pathways are recapitulated by the in vitro systems used, then the fundamental relationship to predict victim DDIs using static **(Equation 4)** or dynamic modeling (Ex: SimCYP) emphasizing F_g and $f_{m,CYPi}$, (Guest et al., 2011), can be applied

$$\frac{AUC'}{AUC} = \frac{F_G'}{F_G} \bullet \frac{1}{\sum_{i}^{n} \frac{fm_{CYPi}}{1+\sum_{j}^{m} \frac{[I]_j}{K_{i,j}}} + \left(1-\sum_{i}^{n} fm_{CYPi}\right)}$$

Equation 4

where [I] is the inhibitor concentration, $K_{i,}$ is the inhibition constant, f_m is the fraction of substrate drug metabolized by P450 enzyme under investigation, ($1–f_{m,CYPi}$) represents clearance via other CYP enzymes and/or renal clearance, F_g and F'_g is the fraction escaping metabolism in the intestine in the absence or presence of inhibitor. **Equation 4** demonstrates the significance of f_m. Inaccuracy in f_m estimates could result in an under-prediction of victim interactions, leading to higher than expected increase in exposure of the probe substrate and potential toxicological events; in contrast, an over-prediction of DDI may suggest an inaccuracy in estimation of f_m and potential missed pathways of disposition of the investigational molecule. The current report discusses one such case study of how lower than predicted victim interactions of investigational

DMD Fast Forward. Published on April 25, 2018 as DOI: 10.1124/dmd.118.080457
This article has not been copyedited and formatted. The final version may differ from this version.

$5HT_6$ antagonist, SAM-760, led to a renewed assessment of the clearance pathways of this molecule using radiolabeled [^{14}C]SAM-760 in human hepatocytes. The metabolism of [^{14}C]SAM-760 **(Figure 1)** in human hepatocytes revealed a previously unidentified and structurally unanticipated pathway which was insensitive to the presence of 1-ABT. Subsequent enzyme mapping of the remaining, 1-ABT sensitive, metabolic disposition via product formation in human hepatocytes verified the magnitude of CYP3A DDI of SAM-760, that was observed in the clinical DDI study in presence of ketoconazole.

SAM-760 was identified as a potent $5HT_6$ antagonist suitable for clinical development. In HLMs, under standard incubation conditions, SAM-760 demonstrated low metabolic turnover and was primarily oxidatively metabolized at the piperazine ring. Substrate depletion experiments of SAM-760 in recombinant P450 isozymes and in HLMs using P450 specific inhibitors suggested that CYP3A was the predominant metabolic isozyme contributing to ~85% of metabolic clearance. Using ketoconazole as the probe CYP3A inhibitor, static equation predicted ~5-fold change in plasma AUC_{0-inf} of SAM-760, suggesting a high likelihood of significant interaction with moderate to strong CYP3A inhibitors. However, in a clinical DDI study when SAM-760 (5 mg, P.O.) was co-administered with ketoconazole (400 mg, P.O.), a modest 1.38-fold increase in mean plasma C_{max} and AUC_{0-inf} of SAM-760 was observed **(Table 3 and Figure 6)**.

This 1.38-fold pharmacokinetic interaction of SAM-760 with ketoconazole was inconsistent with the predicted (~5-fold) change. The lower than predicted interaction with ketoconazole obviated the need to exclude concomitant drugs that may be moderate to strong CYP3A inhibitors. However, this unexpected clinical data suggested that CYP3A may not be the predominant pathway of clearance of SAM-760, and that

substrate depletion experiments of unlabeled SAM-760 in human liver microsomes may have over-estimated its CYP3A contribution. These data also suggested potential role of additional, non-P450 mediated clearance mechanisms of SAM-760. An understanding of all the clearance pathways is an important consideration for defining inclusion and exclusion criteria in later phases of clinical programs.

Therefore, additional investigation was undertaken using radiolabeled [^{14}C]SAM-760, with the label located on the aryl ring adjacent to the sulfonamide group **(Figure 1)**. The position of the label had been selected due to absence of metabolic events on the aryl ring, during incubations of unlabeled SAM-760 in liver microsomes. Due to low turnover of SAM-760 in human liver microsomes and to identify any other missed pathways of metabolism, experiments of [^{14}C]SAM-760 **(Figure 1)** were undertaken in a more comprehensive metabolic system of cryopreserved human hepatocytes; incubates were analyzed using HPLC followed by radio-chromatography and MS/MS. Radio-chromatograms of [^{14}C]SAM-760 incubated in human hepatocytes attributed highest radioactivity to an unexpected, new, high-abundance, broad, highly polar metabolite eluting much earlier than the parent molecule, at ~15.2 min, and corresponding to a *m/z* 143. Exact mass measurements and fragmentation pattern revealed that this polar metabolite may be benzenesulfinic acid, potentially originating from metabolism of the aryl sulfonamide of SAM-760 **(Figure 4)**. In human hepatocytes, this peak contributed to ~43% of total radioactivity attributed to metabolites of SAM-760 and was insensitive to 1-ABT **(Figure 2 and Table 1)**; remaining metabolites were inhibited by 1-ABT.

This observation of benzene sulfinic acid to be the predominant metabolic pathway in human hepatocytes was consistent with a separate investigation of

[^{14}C]SAM-760 in a rat mass balance study. This study also showed that metabolic clearance predominated via biotransformation of the aryl sulfonamide; <10% of total radioactivity was attributed to unchanged SAM-760 in urine and feces confirming that renal and biliary pathways were minor routes of elimination of SAM-760 (data not shown). Overall, predominance of this non-CYP3A mediated metabolic clearance of SAM-760 may explain the lack of significant DDI with ketoconazole, in the clinical DDI study.

The metabolism of aryl sulfonamide benzimidazole group to benzenesulfinic acid was unanticipated and unprecedented. This is intriguing since sulfonamides are metabolically and chemically stable. It has been reviewed (Kalgutkar, 2010) that metabolism of a sulfonamide is not as straight-forward as that of amides and esters, and requires N-hydroxylation as a rate limiting step, under strongly alkaline or anaerobic conditions, resulting in subsequent release of $NO^{\cdot+}$ radical and sulfonic acid metabolite. However, this opportunity does not exist for SAM-760 due to the unavailability of an alpha proton on the benzimidazole nitrogen that constitutes the sulfonamide core. Cleavage of activated sulfonamides by nucleophilic attack of GSH in presence of GSTs and NATs has been reported previously; cleaving of sulfonamides via activation of sulfonamides has been applied as a prodrug strategy for metformin (Larsen and Bundgaard, 1989; Singh et al., 2006; Rautio et al., 2014). GST catalyzed displacement of PNU-109112 has been reported and SAR of activated sulfonamides has been studied (Koeplinger et al., 1999; Zhao et al., 1999). Similarly GSH or cysteine mediated nucleophilic displacement of hetero-aryl substituted sulfonamides has also been reported (Conroy et al., 1984). However, our investigation did not support nucleophilic

displacement of the aryl sulfonamide from the benzimidazole-sulfonamide group of SAM-760 as no GSH or N-acetyl cysteine conjugates of SAM-760 or of its metabolites were observed. Incubation of SAM-760 with GSH in presence of hGST did not form benzene sulfinic acid or GSH/N-Ac conjugates of SAM-760. On the contrary, control incubations of SAM-760 with GSH (no GST added) showed small amounts of benzene sulfinic acid. We proposed that the metabolism of SAM-760 to benzene sulfinic acid may progress non-enzymatically and may be a reduction mediated by thiols like GSH. We confirmed this hypothesis, by a subsequent incubation of SAM-760 with three different thiols: GSH, N-acetyl cysteine, and β-EtSH **(Figure 5)**. Human hepatocytes contain endogenous thiols like cysteine and GSH. Thus it can be hypothesized that under incubation conditions described above, thiols present in human hepatocytes may have cleaved SAM-760 to form benezene sulfinic acid.

The key goal of the current post-hoc investigation was to use in vitro tools to verify the observed CYP3A DDI of SAM-760 in presence of ketoconazole. The in vitro data revealed that predominant metabolic pathway (~43%) in human hepatocytes was non-CYP mediated. Remaining radioactivity **(Table 1)** in human hepatocytes was sensitive to 1-ABT; therefore enzyme phenotyping was performed in human hepatocytes by studying the formation of each of the 1-ABT sensitive metabolites and their inhibition in presence of isozyme specific P450 inhibitors. The fraction of SAM-760 metabolized by each of the major P450 isozymes was calculated using **equations 1-3**. 1-ABT sensitive oxidative metabolites of SAM-760 were primarily formed from CYP3A, with minor contributions from other CYP isoforms 2C19 and 2D6. Using ketoconazole as the probe CYP3A inhibitor and using the *in vitro* human hepatocyte derived f_m

DMD Fast Forward. Published on April 25, 2018 as DOI: 10.1124/dmd.118.080457
This article has not been copyedited and formatted. The final version may differ from this version.

CYP3A (33%), the static equation accurately predicted the observed ~1.38-fold change in AUC_{0-inf} of SAM-760.

This case study illustrates post-hoc investigation of [^{14}C]SAM-760 in human hepatocytes and verification of its observed clinical DDI. In conclusions, SAM-760 was predominantly cleared via novel pathway of metabolism of the aryl sulfonamide group. This novel reaction proceeded non-enzymatically, via thiol mediated reductive cleavage of the aryl sulfonamide yielding benzenesulfinic acid. Identification of this unexpected, non-CYP catalyzed reaction substantiates the use of human hepatocytes to study low turnover compounds, in discovery and development stages. While several methods have been validated and reviewed to study the metabolism of low turnover compounds (Di et al., 2013; Di and Obach, 2015; Hutzler et al., 2015) this manuscript emphasizes the importance of monitoring metabolite formation to accurately identify fractions of metabolism via both CYP and non-CYP pathways and enable assessing DDI risks in clinical development. Finally, in vitro enzyme phenotyping studies of SAM-760 in human hepatocytes provided important insights into explaining the lower than predicted pharmacokinetic interaction of SAM-760 with ketoconazole.

Acknowledgments

The authors would like to acknowledge Douglas Spracklin, Ph.D., Jennifer Liras, Ph.D. for support of the scientific investigations of this manuscript and Michael Coutant., Ph.D. for discussions on pharmaceutical properties of SAM-760. Authors would like to thank Andre Negahban for discussions and guidance on metabolite quantification assay.

Declaration of conflicts of interest

The authors hereby declare no conflicts of interest.

Authorship Contributions:

Participated in research design: Sawant-Basak, Obach, Doran, Tse, Comery.

Conducted experiments: Obach, Doran, Schildknegt, Gao.

Contributed new reagents or analytic tools: Obach, Doran, Schildknegt, Gao.

Performed data analysis: Sawant-Basak, Obach, Doran, Lockwood, Gao, Mancuso, Tse, Comery.

Wrote or contributed to the writing of the manuscript: Sawant-Basak, Obach, Doran, Lockwood, Mancuso, Tse.

References

Conroy CW, Schwam H, and Maren TH (1984) The nonenzymatic displacement of the sulfamoyl group from different classes of aromatic compounds by glutathione and cysteine. *Drug metabolism and disposition: the biological fate of chemicals* **12:**614-618.

Di L, Atkinson K, Orozco CC, Funk C, Zhang H, McDonald TS, Tan B, Lin J, Chang C, and Obach RS (2013) In vitro-in vivo correlation for low-clearance compounds using hepatocyte relay method. *Drug metabolism and disposition: the biological fate of chemicals* **41:**2018-2023.

Di L and Obach RS (2015) Addressing the challenges of low clearance in drug research. *The AAPS journal* **17:**352-357.

Foley AG, Hirst WD, Gallagher HC, Barry C, Hagan JJ, Upton N, Walsh FS, Hunter AJ, and Regan CM (2008) The selective 5-HT6 receptor antagonists SB-271046 and SB-399885 potentiate NCAM PSA immunolabeling of dentate granule cells, but not neurogenesis, in the hippocampal formation of mature Wistar rats. *Neuropharmacology* **54:**1166-1174.

Guest EJ, Rowland-Yeo K, Rostami-Hodjegan A, Tucker GT, Houston JB, and Galetin A (2011) Assessment of algorithms for predicting drug-drug interactions via inhibition mechanisms: comparison of dynamic and static models. *British journal of clinical pharmacology* **71:**72-87.

Haydar SNA, Patrick Michael; Yun, Heedong; Robichaud, Albert Jean (2009) 1-(Arylsulfonyl)-4-(piperazin-1-yl)-1H-benzimidazole compounds as 5-

hydroxytryptamine-6 receptor ligands and their preparation and use in the treatment of diseases.

Hirst WD, Stean TO, Rogers DC, Sunter D, Pugh P, Moss SF, Bromidge SM, Riley G, Smith DR, Bartlett S, Heidbreder CA, Atkins AR, Lacroix LP, Dawson LA, Foley AG, Regan CM, and Upton N (2006) SB-399885 is a potent, selective 5-HT6 receptor antagonist with cognitive enhancing properties in aged rat water maze and novel object recognition models. *European journal of pharmacology* **553:**109-119.

Hutzler JM, Ring BJ, and Anderson SR (2015) Low-Turnover Drug Molecules: A Current Challenge for Drug Metabolism Scientists. *Drug metabolism and disposition: the biological fate of chemicals* **43:**1917-1928.

Kalgutkar AS, Jones R, and Sawant AD (2010) Sulfonamide as an essential functional group in Drug Design, in: *Metabolism, Pharmacokinetics, and Toxicity of Functional Groups: Impact of chemical building blocks on ADMET* (Smith DA ed), pp 210-275, Royal Society of Chemistry, Cambridge, UK.

Koeplinger KA, Zhao Z, Peterson T, Leone JW, Schwende FS, Heinrikson RL, and Tomasselli AG (1999) Activated sulfonamides are cleaved by glutathione-S-transferases. *Drug metabolism and disposition: the biological fate of chemicals* **27:**986-991.

Kotegawa T, Laurijssens BE, Von Moltke LL, Cotreau MM, Perloff MD, Venkatakrishnan K, Warrington JS, Granda BW, Harmatz JS, and Greenblatt DJ (2002) In vitro, pharmacokinetic, and pharmacodynamic interactions of ketoconazole and

midazolam in the rat. *The Journal of pharmacology and experimental therapeutics* **302:**1228-1237.

Larsen JD and Bundgaard H (1989) Prodrug forms for the sulfonamide group. IV. Kinetics of hydrolysis of N-sulfonyl pseudourea derivatives. *Acta pharmaceutica Nordica* **1:**31-40.

Liu KG, Robichaud AJ, Greenfield AA, Lo JR, Grosanu C, Mattes JF, Cai Y, Zhang GM, Zhang JY, Kowal DM, Smith DL, Di L, Kerns EH, Schechter LE, and Comery TA (2011) Identification of 3-sulfonylindazole derivatives as potent and selective 5-HT(6) antagonists. *Bioorganic & medicinal chemistry* **19:**650-662.

Maher-Edwards G, Dixon R, Hunter J, Gold M, Hopton G, Jacobs G, Hunter J, and Williams P (2011) SB-742457 and donepezil in Alzheimer disease: a randomized, placebo-controlled study. *International journal of geriatric psychiatry* **26:**536-544.

Rautio J, Vernerova M, Aufderhaar I, and Huttunen KM (2014) Glutathione-S-transferase selective release of metformin from its sulfonamide prodrug. *Bioorganic & medicinal chemistry letters* **24:**5034-5036.

Singh SK, Vobbalareddy S, Kalleda SR, Casturi SR, Mullangi R, Ramanujam R, Yeleswarapu KR, and Iqbal J (2006) N-acylated sulfonamide sodium salt: a prodrug of choice for the bifunctional 2-hydroxymethyl-4-(5-phenyl-3-trifluoromethyl-pyrazol-1-yl) benzenesulfonamide class of COX-2 inhibitors. *Bioorganic & medicinal chemistry letters* **16:**3921-3926.

Vuppugalla R, Zhang Y, Chang S, Rodrigues AD, and Marathe PH (2012) Impact of nonlinear midazolam pharmacokinetics on the magnitude of the midazolam-ketoconazole interaction in rats. *Xenobiotica* **42:**1058-1068.

Zhao Z, Koeplinger KA, Peterson T, Conradi RA, Burton PS, Suarato A, Heinrikson RL, and Tomasselli AG (1999) Mechanism, structure-activity studies, and potential applications of glutathione S-transferase-catalyzed cleavage of sulfonamides. *Drug metabolism and disposition: the biological fate of chemicals* **27:**992-998.

DMD Fast Forward. Published on April 25, 2018 as DOI: 10.1124/dmd.118.080457
This article has not been copyedited and formatted. The final version may differ from this version.

Figure legends:

Figure 1. Chemical structures of [^{14}C]SAM-760 and [D_8]WYE-103760.

Figure 2. HPLC radio-chromatograms of metabolites of [^{14}C]SAM-760 in human hepatocyte incubations. [^{14}C]SAM-760 (10 µM) was incubated with human hepatocytes for 4 hr without (red top trace) or with (green middle trace) 1 mM 1-ABT. The blue bottom trace is a control incubation at t=0h. Numbers designate the individual metabolites listed in **Table 1**. Peaks designated with "i" represent radiochemical impurities and the large peak eluting at ~35 min is the unchanged parent drug (SAM-760).

Figure 3. Proposed metabolic pathways of SAM-760 observed in human hepatocytes.

Figure 4. Comparison of elution profile of benzenesulfinic acid under identical chromatographic conditions. Top panel shows benzene sulfinic acid as observed in the radio-chromatogram of SAM-760, on incubation of [^{14}C] SAM-760 in human hepatocytes; lower panel is the extraction ion chromatogram of benzene sulfinic acid (under negative ion chromatogram of *m/z* 141). Arrows indicate the corresponding peaks at ~15 min.

Figure 5. Negative ion electrospray extracted ion chromatograms of benzene sulfonate ion (*m/z* 141). The panels (top to bottom) are XICs from incubation of SAM-760 in buffer with no thiols added (control), GSH, N-Acetyl Cysteine, and β- EtSH.

Figure 6. Mean (+/-SEM) plasma concentrations of SAM-760 following a single oral 5 mg dose (red trace) or after 400 mg QD ketoconazole administered for 2 weeks (blue trace).

DMD Fast Forward. Published on April 25, 2018 as DOI: 10.1124/dmd.118.080457
This article has not been copyedited and formatted. The final version may differ from this version.

Tables

Table 1. Summary of proposed metabolites observed in radio- chromatogram (red trace in **Figure 2**) and % of metabolism of SAM-760 in human hepatocytes.

Table 2. Cumulative contribution of P450 isozymes, to each of the 1-ABT-sensitive metabolic pathways of SAM-760 in human hepatocytes, determined using **equations 1-3**.

DMD Fast Forward. Published on April 25, 2018 as DOI: 10.1124/dmd.118.080457
This article has not been copyedited and formatted. The final version may differ from this version.

Peak #	R_t (min)	m/z	Putative ID	% of total radioactivity from metabolites	1-ABT Sensitive?
1	15.2	143	Benzenesulfinic acid	43	No
2	~18	ND	Unknown	6.3	No
3	19.7	549	glucuronide of peak 5	4.5	Yes
4	~27	ND	Unknown	1.9	Yes
5	30.1	373	Hydroxyl on methyl benzimidazole	1.3	Yes
6	33.0	373	Hydroxyl on methyl benzimidazole	1.5	Yes
SAM-760	35.1	357	SAM-760	N/A	N/A
7	36.7	389	carboxylic acid	12	Yes
8	38.5	549	glucuronide of peak 9	7.2	Yes
9	39.1	373	Hydroxylamine of piperazine	1.3	Yes
10	41.3	369	unknown	2.0	Yes
11	41.8	389	carboxylic acid	1.7	Yes
12	45.3	437	sulfamic acid on piperazine	4.5	No
13	46.6	373	N-Acetyl	4.8	Yes
14	48.8	288	cleaved piperazine	5.8	Yes
15	50.0	346	piperazine oxidation	2.6	Yes

DMD Fast Forward. Published on April 25, 2018 as DOI: 10.1124/dmd.118.080457
This article has not been copyedited and formatted. The final version may differ from this version.

Peak # in Figure 2	HPLC R_t (min)	MRM transition	CYP2C19	CYP2D6	CYP3A
Peak 3	1.18	549→232			4.3%
Peak 5	1.46	373→232		0.47%	0.83%
Peak 6	1.53	373→174	0.06%		0.90%
Peak 7	1.66	389→160	4.5%		10%
Peak 8	1.69	549→232			3.3%
Peak 9	1.70	373→232			0.69%
Peak 10	1.91	369→228	0.85%		1.1%
Peak 11	1.91	389→248	0.80%		0.90%
Peak 13	2.0	373→232			3.4%
Peak 14	2.06	288→147.1			5.5%
Peak 15	2.04	346→160.1			2.4%
SAM-760 Fraction Metabolized (f_m)	NA	NA	6.3%	0.47%	33%

DMD Fast Forward. Published on April 25, 2018 as DOI: 10.1124/dmd.118.080457
This article has not been copyedited and formatted. The final version may differ from this version.

Table 3. Geometric mean (%CV) and ratio of PK parameters following a single oral 5 mg dose of SAM-760, QD either alone or when co-administered with 400 mg ketoconazole, QD.

Treatment (N=12)	**C_{max} (ng/mL)**	**AUC_{0-inf} (ng*h/mL)**
SAM-760, 5 mg	3.43 (30)	154.5 (26)
SAM-760, 5 mg +Ketoconazole, 400 mg	4.47 (20)	213.7 (18)
[SAM-760+Ketoconazole]/[SAM-760]	1.30	1.38

DMD Fast Forward. Published on April 25, 2018 as DOI: 10.1124/dmd.118.080457
This article has not been copyedited and formatted. The final version may differ from this version.

Scheme 1.

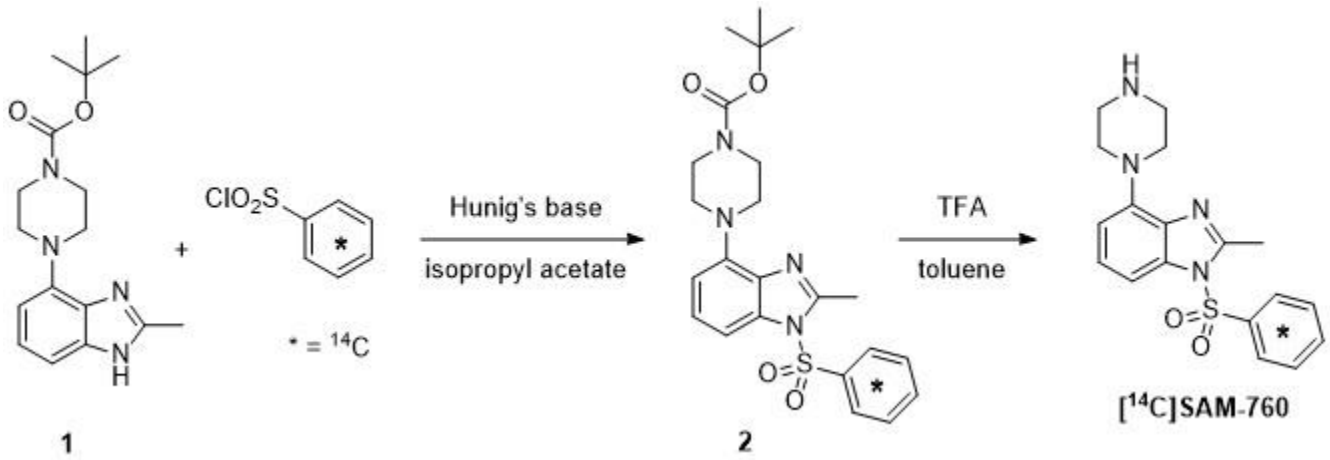

DMD Fast Forward. Published on April 25, 2018 as DOI: 10.1124/dmd.118.080457
This article has not been copyedited and formatted. The final version may differ from this version.

Figures:

Figure 1.

SAM-760

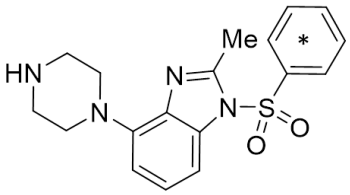

D_8 WYE-103760

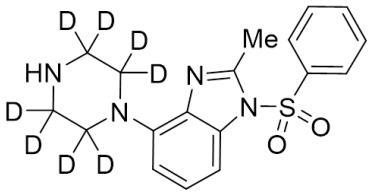

DMD Fast Forward. Published on April 25, 2018 as DOI: 10.1124/dmd.118.080457
This article has not been copyedited and formatted. The final version may differ from this version.

Figure 2.

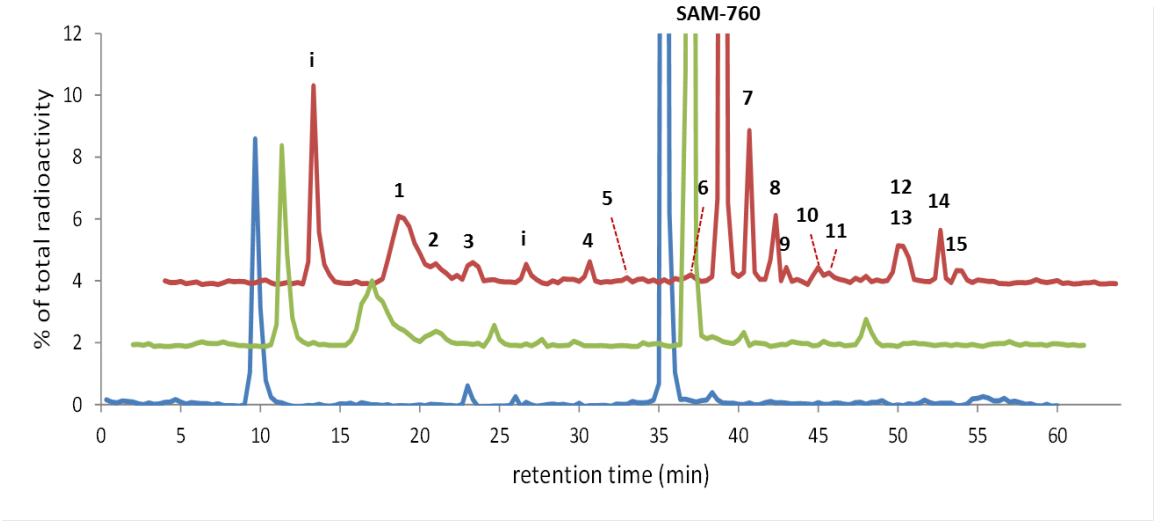

DMD Fast Forward. Published on April 25, 2018 as DOI: 10.1124/dmd.118.080457
This article has not been copyedited and formatted. The final version may differ from this version.

Figure 3.

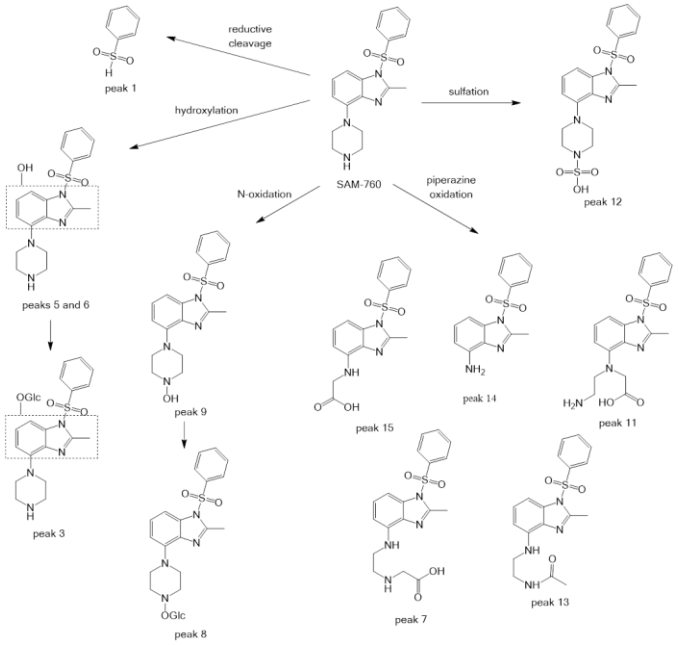

DMD Fast Forward. Published on April 25, 2018 as DOI: 10.1124/dmd.118.080457
This article has not been copyedited and formatted. The final version may differ from this version.

Figure 4.

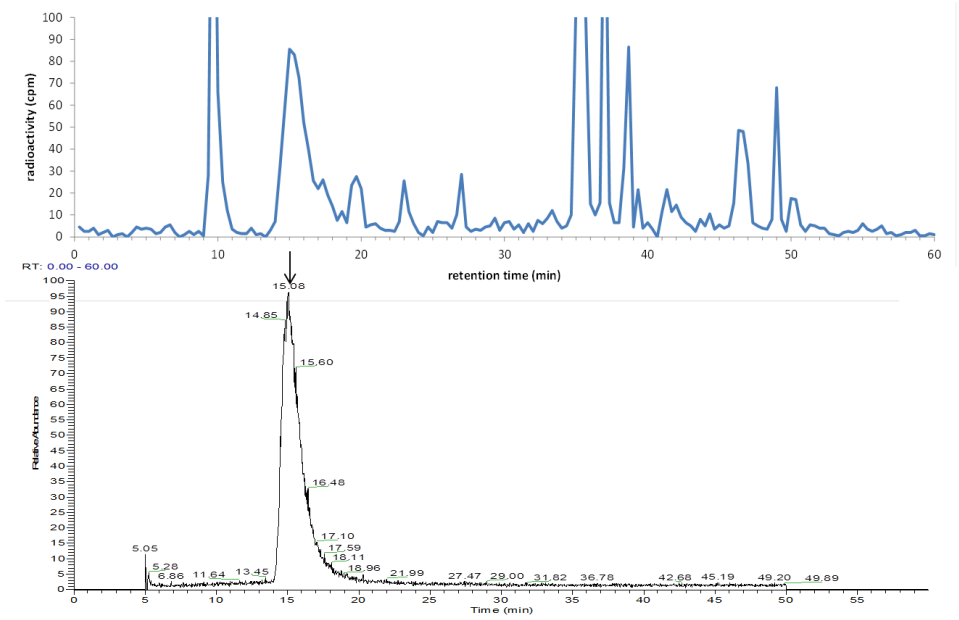

DMD Fast Forward. Published on April 25, 2018 as DOI: 10.1124/dmd.118.080457
This article has not been copyedited and formatted. The final version may differ from this version.

Figure 5.

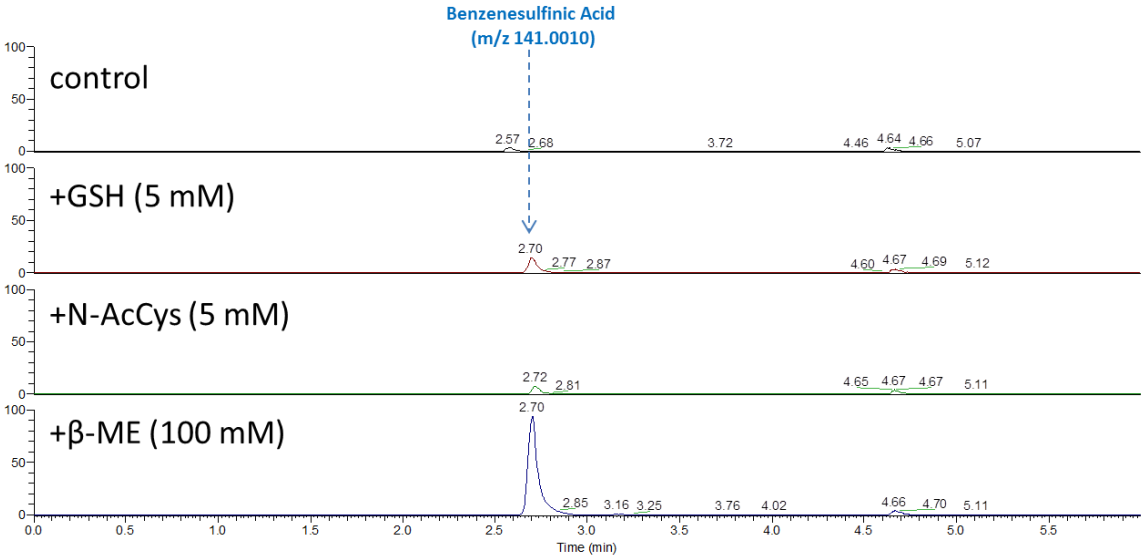

DMD Fast Forward. Published on April 25, 2018 as DOI: 10.1124/dmd.118.080457
This article has not been copyedited and formatted. The final version may differ from this version.

Figure 6.